Int J Clin Exp Pathol 2011;4(4):385-402
www.ijcep.com /IJCEP1104007

Original Article

Proteasome degradation of brain cytosolic tau in Alzheimer's disease

Samuel S. Yen

Department of Neuroscience, Mayo Clinic College of Medicine, 4500 San Pablo Road, Jacksonville, FL, USA.

Received April 10, 2011; accepted April 23, 2011; Epub April 28, 2011; published April 30, 2011

Abstract: The proteasomal degradation of cytosolic, phosphorylation-independent tau in human brains is potentially linked to the pathogenesis of neurofibrillary pathology in Alzheimer's disease (AD). Previous studies showed that the active 20S proteasome core degrades recombinant tau effectively, which prompted this study to determine if there was evidence of proteasomal degradation of tau in human brain with a range of neurofibrillary pathology. Cytosolic proteins from temporal cortex were isolated from 30,000xg supernatants by resolving in size-exclusion chromatography for assay of tau and proteasomal subunits by Western blots. Levels of tau and proteasome subunits varied from case to case, with a significant inverse correlation between the levels of tau and 20S β-subunits, and between 70-kDa tau and 11S β-subunits, suggesting that tau is a proteasomal substrate. The inability to detect tau in western blots on cases without neurofibrillary pathology is consistent with the hypothesis that the proteasome is capable of degrading normal tau with an intact projection domain at the amino-terminal end; however, as proteasomal function becomes impaired during aging, tau clearance is impeded. Tau accumulates in progressively larger and more heterogeneous forms in brains with neurofibrillary pathology. Under normal conditions, non-proteasomal proteases are capable of digesting recombinant-tau from both the amino- and carboxyl-terminal ends toward the mid-section, but are lack of chaperon-like activity to unfold carboxyl-terminal truncated tau accumulated in AD. Our results support the hypothesis that failure of proteasomal and non-proteasomal proteolytic clearance mechanisms leads to tau accumulation and progressive neurofibrillary degeneration in AD.

Keywords: Alzheimer's disease, immunoblotting, neurofibrillary, PHF-tau, proteasome, size- exclusion chromatography, tau

Introduction

Alzheimer's disease (AD) is the most common neurodegenerative disorder of the elderly and is characterized by clinical symptoms of cognitive impairment and memory loss leading eventually to dementia [1]. Age is the major risk factor. The hallmark pathologic characteristics of AD are amyloid deposition, progressive neuronal loss and neurofibrillary tangles (NFTs) composed of tau protein [2, 3], ultrastructurally composed of paired helical filaments (PHFs) [4]. PHFs are resistant to protease digestion [2, 4], but are partially soluble in detergents, such as sodium dodecyl sulfate (SDS) [5] and 1% sarkosyl [6]. Both NFTs and PHFs are composed of the microtubule (MT)-associated protein tau, which is normally a soluble, unfolded cytosolic protein [7]. Tau promotes assembly and stabilizes MT [8] for diverse homeostatic neuronal functions, such as the axoplasmic transport of organelles and proteins [9, 10]. Specific forms of tau are associated with nuclear double-stranded DNA and may play a role in gene regulation [11].

Newly synthesized tau may occasionally escape quality control mechanisms of the endoplasmic reticulum (ER) and become misfolded. Both ribosomal-defective tau and tau targeted for turnover are subject to immediate degradation. The exact mechanisms of tau degradation in the human brain are unknown, but have been demonstrated *in vitro* using the 20S proteasome core [12] and non-proteasomal proteases (proteases), such as cathepsin-D [13], caspases [14] and calpain 1 [15].

The proteasome system is expressed in normal

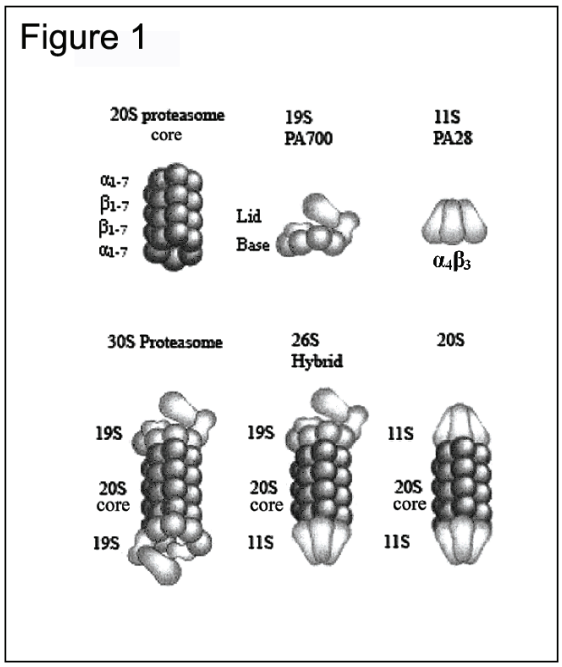

Figure 1. The proteasome system.The proteasome consists of 20S proteasome core, 19S proteasome and 11S proteasome [44]. 20S core conjugated at both ends by two 19S proteasomes or 11S proteasomes to form 30S proteasom for degradation of tau to tau-peptides and 20S proteasome for digestion of tau-peptides to amino acids, respectively. 26S hybrid proteasome, 19S-20S core-11S, digests tau to antigen peptides and amino acids directly.

brains, but protease functional impairment accompanies aging and neurodegenerative disease [16]. In the absence of proteasome, non-proteasomal proteases degrade tau primarily at the carboxyl-terminus because the amino-terminus of tau has a functional, specifically configured projection domain.

The proteasome, a compartmentalized multicatalytic complex (see reviews [17-19]), consists of a 20S proteasome core (20S core), as well as 11S and 19S proteasome regulatory components. The core is a hollow cylinder consisting of four stacked rings, which maintain the unfolded structure of the substrate and degrade the proteins completely. The $\beta_5$chymotrypsin-like (chymotrypsin), $\beta_2$trypsin-like (trypsin) and $\beta_1$caspase-like proteases, as well as four inactive subunits form the β-ring. The β-subunits interact diagonally and overlap [17, 18] with their counterparts [20-23] to cleave various peptide bonds [21-25] for allosteric proteolysis [26]. *In addition, the* β-proteases *must* integrate an α-ring template to form a core for most effective substrate degradation [22]. The proteasome degrades recombinant-tau by repeated removal of short portions from both the N- and C-termini towards the middle of the protein [12].

The 20S core can interact with two to one 19S proteasome activator (PA) 700 particles and/or 11S PA28 particles to form the 30S, 26S hybrid and 20S proteasomes (**Figure 1**). Regulatory particle (RP) ATPases 1-6 (Rpt1-6) in 19S PA700 have chaperone-like activity. RP non-ATPase protein 10 (Rpn10) upon binding to ubiquitinated chains repairs damaged proteins ready for unfolding by Rpt1-6 [19]. Rpt1-6, Rpn10 and Rpn2 collectively facilitate the entry of substrate via the proteasome orifice of the α-subunits to enzyme cavity formed by the two β-rings [27].

Tau aggregates are found more often in aged than in young brains, which suggests that incomplete degradation of tau contributes to the pathogenesis of AD. The approximate five-day half-life of tau protein [28] and the effective degradation of purified 20S core on recombinant (r)-tau [12] prompted this study. Cytosolic tau, proteasome subunits and 20S β-proteases were enriched in human brain samples by size-exclusion chromatography and their levels analyzed with immunoblots. Levels of total tau and 20S β-subunits as well as 70-kDa tau and 11S β-subunits were measured. Inability to detect tau on immunoblots was used as the index of complete tau degradation. Simultaneous measurement of 20S α-ring components was used to determinate whether the 20S β-proteases were integrated successfully into the proteasome.

Materials and methods

Case material

Temporal cortex tissue was obtained from 16 cases from the brain bank at Mayo Clinic Jacksonville, Florida including some patients who had been followed longitudinally in the Mayo Clinic Alzheimer Disease Research Center (NIH P50-AG16574). The cases included four non-AD controls and six cases of early AD and six cases of advanced AD.

Size exclusion chromatography of cytosolic proteins

One gram of gray matter from temporal cortex, a

cortical region vulnerable to tau pathology in aging and AD, was dissected and homogenized (1:5, w/v) in a proteolysis buffer composed of 50 mM HEPES at pH 7.5, with 5 mM $MgCl_2$, 20% glycerol, 10 μg/ml protease inhibitor cocktail (PIC) for mammalian cell extracts (P8340, Sigma Chemical, St. Louis, MO) and phosphatase inhibitor cocktail (PPIC) (containing 5 mM sodium pyrophosphate; 30 mM of both sodium fluoride and β-glycerophosphate). The homogenates were centrifuged at 30,000 x g for one hour at 4°C to produce a supernatant that was processed as follows.

A Superose 6 (Amersham Biosciences) column (inner diameter 1.5 cm x 42 cm) was packed and equilibrated with two column volumes of elution medium that was composed of 20 mM HEPES at pH 7.5, with 1 mM each of EGTA and EDTA, 5 mM DTT, 10% glycerol, PIC and PPIC. In addition, a high molecular weight calibration kit (Amersham Biosciences), highly purified human PHF preparations (provided by Dr. Peter Davies, Albert Einstein College of Medicine) and full-length recombinant tau were used to calibrate each protein's Stokes radius (Rs) and MW values in the fraction. The total volume of 30,000 x g supernatant from each case was loaded on the pre-equilibrated size-exclusion chromatography (SEC) at room temperature (RT) and proteins resolved in 0.9 ml fractions were collected and stored at -20°C until used.

Measurement of cytosolic tau and proteasome 20S α- and β-subunits

Levels of tau, 20S α-subunits and β-subunits, and 11S α-subunits and β-subunits in all fractions were analyzed by 10% SDS-PAGE WB and found in fraction (F) F28-F75. Eighteen microliters of eluate were loaded per lane. To assure absence of tau and proteasome subunits in cases with no detectable (ND) tau or proteasome subunits, more eluate was loaded and the blots were over-exposed on x-ray film. A ladder of MW markers (Bio Rad, Hercules, CA) and six r -tau isoforms of 47-68-kDa [15] were added in each blot as calibration standards and positive controls. In addition, a 100,000 x g supernatant purified from frontal cortex of a case of AD with severe neurofibrillary degeneration was used as a control for normalizing protein levels. This preparation had the typical 3-bands of abnormal hyperphosphorylated tau in AD migrating at about 55-, 64- and 68-kDA. Amino-terminus, two mid-sections, and carboxyl-terminus of tau were detected on blots with antibody E1 (aa 19-33) [29], P44 (aa 162-178) and P46 (aa 350-370) [30-32] and Tau46 (aa 404-441) [33]. These antibodies were diluted as follows: E1 at 1:2,000, P44 at 1:1,500, P46 at 1:1,000, and Tau46 at 1:20,000 to produce identical blot intensities using r-tau as a standard.

Immunoblotting with P-tau antibodies, including AT270 (aa 181), AT180 (aa 231) and AT8 (aa 202/205) from Innogenetics, Gent, Belgium, and CP13 (aa 202), PG5 (aa 422) and PHF1 (aa 396/404) from Peter Davies, Albert Einstein College of Medicine, was examined. The monoclonal antibody PHF1 yielded the broadest P-tau blots and the strongest intensity of the antibodies tested. Thus, PHF1 diluted at 1:2,000 was used to detect P-tau.

20S α-subunits and β-subunits were blotted using monoclonal IgG1 antibody Clones P32 and P27 [34] (Research Diagnostics, Flanders, NJ). 11Sα-subunits and β-subunits were probed by polyclonal antibody PA28α and PA28β, respectively [35]. Blots of 19S Rpt1-6 were performed using monoclonal antibodies to Rpt1, Rpt4 and Rpt5, and polyclonal antibodies to Rpt2, Rpt3 and Rpt6 (Biomol International, Plymouth Meeting, PA).

Photoimages were generated using ECL+ system (GE Healthcare) and analyzed by densitometry in the MCID system (Image Research, ON, Canada). Background deduction remained constant throughout the experiments. The 70-kDa tau was defined as tau immunoreactive species migrating on the blot above the largest 4R-2N recombinant-tau (68-kDa). Levels of the proteins were the sum of positive fractions. The total tau was the sum of immunoreactivity of all tau species in the blot.

Measurement of 20S β-protease activity

Levels of three 20S β-proteases in each case were analyzed by fluorescence substrate assay [36]. The specific substrates were Succinyl-LL-VT-AMC, Boc-AA-AMC and Z-LL-E-βNA for chymotrypsin, trypsin and caspase activity, respectively. The same substrate was used to measure the β-protease activity in 20S core and 19S-activated 20S core. The specific proteasome inhibitors MG132 and lactacystin (Biomol International, Plymouth Meeting, PA) were also included in the duplicates to differentiate the level of proteasome from non-proteasome activ-

Table 1. Summary of case material

Class	Case #	Age	Sex	PMI	Braak NFT stage	Other pathology
non-AD	1	64	M	NA	0	Corticospinal tract degeneration
	2	46	F	NA	0	Upper and lower motor neuron degeneration
	3	80	F	11	III	Grains & cerebrovascular lesions
	4	95	F	13	III	Diffuse plaques & brainstem Lewy bodies
	5	95	F	25	II	None
Early AD	6	87	F	5	I-II	Cerebrovascular lesions
	7	85	F	7	V	Neuritic plaques
	8	89	M	6	IV	Neuritic plaques & cerebrovascular lesions
	9	103	F	2	V	Neuritic plaques & cerebrovascular lesions
AD	10	94	M	4	III	None
	11	98	F	19	IV-V	Diffuse plaques & cerebrovascular lesions
	12	89	F	13	III	None
	13	93	F	19	VI	Neuritic plaques & brainstem Lewy bodies
	14	94	F	22	V	Neuritic plaques
	15	102	F	17	VI	Neuritic plaques
	16	86	F	8	III	Neuritic plaques, grains& cerebrovascular lesions

Braak NFT stage assigned based upon counts with thioflavin S fluorescent microscopy as part of routine diagnostic neuropathology. F = female; M = male; NA = not available; PMI = postmortem interval (in hours).

ity. At the beginning, effective concentrations of peptide substrates and specific inhibitors on the respective enzyme assays were tested. Using 100 μM of substrate or 100 μM of a specific inhibitor was found to produce the maximal fluorescence products and the complete inhibition of the substrate degradation, respectively. Hence, both classes of chemicals at 100 μM were used and prepared in DMSO for a final medium concentration at less than 1%.

Duplicates of 100 μl of eluate from F28-75 were prepared in a 96-well fluorescence plate (Corsar, Corning Inc, Corning, NY) with minimal background interference. The samples with vehicle or specific inhibitor were incubated at 37° C for 15 min with slow vortexing. After the addition of fluorescence substrates, the plate received the same treatment for one hour. In the end, an equal volume of 2% SDS in 20 mM HEPES at pH 7.5 was added to terminate the enzyme activity and to preserve the fluorescent products. Both excitation/emission signals for both chymotrypsin and trypsin activity were read at 380/460 nm and caspase activity at 335/410 nm in a Spectra Max Gemini XS spectrophotometer (Molecular Devices, Sunnyvale, CA). The net 20S β-protease activity was the difference between the control where only vehicle was added and treatment with the specific 20S inhibitor. Each index level of each β-protease was the sum of positive fractions that fluctuated greatly. The total index level of 20S β-proteases was the sum of chymotrypsin, trypsin and caspase activity.

Case 1, a middle aged adult with short postmortem interval and no neurofibrillary pathology, had a normal proteasome expression profile with antibodies to the various proteasome subunits. To compare protease levels between the 16 cases, all values were divided by the levels in Case 1 and expressed as a ratio.

Statistical analysis

Non-parametric Kendall's rank correlation, analysis of variance and regression correlation were performed (StatsDirect, Altrincham, Cheshire, UK), and $P<0.05$ was considered significant.

Results

The sixteen cases used in this study included controls with no amyloid plaques or neurofibrillary pathology based upon thioflavin S fluorescent microscopy (Case 1), controls that had a range of low density neurofibrillary pathology, some with diffuse amyloid plaques (Cases 2-4) as well as cases with a range of neurofibrillary pathology, including cases with moderate to advanced neurofibrillary pathology with amyloid and neuritic type cortical plaques. For the sake of this study, the latter are classified as "early AD" (Cases 5-10) and "AD" (Cases 11-16). The demographics of the case material are summa-

Table 2. Tau and proteasome 20S subunits levels

		20S subunits		Tau				P-tau
Class	#	α-	β-	Amino-terminus E1	Mid-section P44	Mid-section P46	Carboxyl-terminus Tau46	PHF1
Non-AD	1	1.890	4.325	ND	ND	ND	ND	ND
	2	5.765	2.380	0.015	ND	ND	ND	ND
	3	0.835	0.345	0.070	ND	ND	ND	0.190
	4	0.150	1.125	0.050	0.010	0.005	ND	ND
	5	0.145	0.015	0.460	0.230	ND	ND	ND
	6	0.145	0.045	0.169	0.053	0.020	ND	ND
Early-AD	7	1.185	ND	1.060	0.140	0.045	ND	ND
	8	0.049	0.350	0.165	0.045	0.035	ND	0.220
	9	0.905	0.090	0.190	0.025	0.125	ND	0.185
	10	0.185	0.570	0.230	0.140	ND	ND	0.205
	11	0.190	0.490	0.310	0.090	0.040	0.110	0.175
	12	0.735	0.150	0.185	0.065	0.045	0.010	0.130
AD	13	0.690	0.275	0.440	0.285	0.130	0.025	0.415
	14	1.770	0.750	0.425	0.130	0.085	0.025	0.750
	15	2.095	0.225	0.445	0.190	ND	ND	1.645
	16	0.945	ND	0.890	0.155	0.295	ND	6.615

Tau amino-terminus, two mid-sections, and carboxyl-terminus were blotted using antibody E1, P44 and P46, and Tau46, and P-tau was detected by PHF1 antibody. 20S α-subunits and β-subunits were proved by p32 and p27 antibody. The levels (AU) were determined by densitometry. ND = not detectable. G: gender; M: male.

rized in **Table 1**.

Tau and proteasomal components in controls

Case 1, deceased at age 64, was younger than all but Case 2; the average age for the other cases was 93 years (**Table 1**). The 20S single-band α- and β-subunits, and 11S α- and β-subunits were resolved in broad fractions and expressed at 1.89AU, 4.33AU (**Table 2**), and 1.10AU, 1.20AU (**Table 3**), respectively. Tau was not detectable (ND) with overloading the gel and overexposing the film. This was taken to indicate that tau underwent complete proteasomal degradation (**Figure 2A**). 11S double-band α-subunits consisted of apparent 90-kDa trimers and 60-kDa dimers and lacked 30-kDa monomers, whereas single-band β-subunits contained trimers, dimers and monomers. Both 11S subunits were expressed at high levels, which would be expected to be capable of activating the 20S core to obtain complete degradation of tau-peptides, consistent with ND 70-kDa tau (**Figure 3A**).

Case 1 also fully expressed regulatory elements Rpt1-6 (**Figure 4**). Rpt1 was detected as a double-band of subunits from 45-42-kDa and from 63-60-kDa. Rpt2 was composed of four subunits at 68, 62, 58 and 50-kDa in series of variable lengths. Rpt3 subunits at 45-kDa and Rpt4 subunits at 46-kDa were distributed very widely. Rpt5 were single-band subunits at 50-kDa and 42-kDa with a minor 68-kDa subunit chain that spanned seven fractions. Rpt6 was detected as single-band at 48-kDa resolved in 17 fractions. Thus, Case 1 was considered to have normal proteasome expression profile for the purposes of comparison.

Case 2, age 46, had a fractional accumulation of undigested 70-kDa tau at 0.005 AU that contained tau with intact N-terminus. The 20S α-subunits were markedly upregulated, as shown by two overlapping double-bands at 300% the level of Case 1, but the β-subunits were down regulated to 55% of Case 1 only. In addition, the 11S α-subunits were down regulated to 0.60 AU, or 64% of Case 1, and contained single-band dimers without monomers. The β-subunit was expressed at 0.77 AU, also at 64% of Case 1, and included dimers, trimers, and smaller MW species, as well as monomers (**Figure 3A, Table 2**). Case 2 had the highest expression levels of Rpt1, Rpt2, Rpt4, and Rpt5 of the 15 diseased cases, but a very low level of Rpt3 and a 33% level of Rpt6 of Case 1. Rpt1 was over expressed as an almost fused double-band at 45-42-kDa as a long series and a short one at 63-60-kDa. Rpt2 was a long series at 55-52-

Table 3. 70-kDa tau and proteasome 11S subunit levels

		70-kDa					11S proteasome					
		Tau				P-tau	α-subunits			β-subunits		
Class	Case	Amino-terminus E1	Mid-section P44	Mid-section P46	Carboxyl-Terminus Tau46	PHF1	90-kDa	60-kDa	30-kDa	90-kDa	60-kDa	30-kDa
Non-AD	1	ND	ND	ND	ND	ND	0.625	0.475	ND	0.925	0.535	0.260
	2	0.005	ND	ND	ND	ND	0.185	0.415	ND	0.760	0.360	0.355
	3	0.055	ND	ND	ND	0.250	ND	ND	0235	ND	ND	0.020
	4	0.045	ND	ND	ND	ND	ND	0.235	ND	ND	0.280	0.260
	5	0.070	ND	ND	ND	ND	ND	ND	0.110	ND	ND	0.160
	6	0.070	0.020	ND	ND	ND	ND	ND	0.065	ND	ND	0.008
Early AD	7	0.145	0.010	ND	ND	ND	ND	ND	0.335	ND	ND	0.400
	8	ND	ND	0.025	ND	0.100	ND	ND	0.240	ND	ND	ND
	9	0.010	ND	0.015	ND	0.050	ND	ND	0.915	ND	ND	0.160
	10	0.230	0.045	ND	ND	0.075	ND	ND	0/030	ND	ND	0.035
	11	0.120	0.109	ND	ND	0.090	ND	ND	0.125	ND	ND	0.190
	12	0.155	0.055	0.090	0.025	0.120	ND	ND	1.405	ND	ND	ND
AD	13	0.100	0.110	0.085	ND	0.445	ND	ND	1.300	ND	ND	0.040
	14	0.185	0.065	ND	ND	0.260	ND	ND	3.315	ND	ND	0.160
	15	ND	0.140	ND	ND	0.430	ND	ND	ND	ND	ND	ND
	16	0.140	ND	ND	ND	0.700	ND	ND	1.330.	ND	ND	0.125

Phosphorylation-independent tau (tau), P-tau and 11Sα-subunits and β-subunits were blotted. The 70kDa tau likely, the aggregates of undigested tau peptides, was determined (AU) by dissecting from the blots at a level above the 4R-2N isomer at 68-kDa. ND = not detectable. The 11Sα-subunits and β-subunits consist of 90-kDa trimers, 60-kDa dimers and 30-kDa monomers. Two oligomer β-subunits are stimulatory and the monomer β-subunit is inhibitory in function.

kDa and a short chain at 63-60-kDa of severely fused double-band subunits. Rpt3 subunits at 45-kDa were down regulated to only 2% of Case 1 and resolved narrowly in SEC. Rpt4 subunits at 46-kDa were expressed as a single band resolved very broadly, which was very strong in the center and weak at both ends, with a short chain of subunits at 28-kDa that spanned 13 fractions. Rpt5 contained a long double-band subunit series at 50-kDa underneath a medium subunit series at 76-kDa. Rpt6 was at a fraction of Case1. Thus, Case 2 had one to two-fold stronger expression of Rpt1, 2, 4 and 5, and very weak Rpt3 and weak Rpt6 expressions than in Case 1 (**Figure 4**). The levels of Rpt1-6 were mismatched and unbalanced. The data showed the onset of proteasome abnormality and tauopathy.

Case 3 had undigested tau including a short chain of 70-kDa tau at 0.070 AU and a very long series of 70-kDa P-tau at 0.190 AU, with both proteins containing the amino-terminus. The 20S α-subunits and β-subunits were downregulated to 7% and 8%, respectively, of Case 1 (**Figure 2A**), and 11S α-subunits and β-subunit were expressed as monomers at 0.235 AU and 0.02 AU, respectively (**Figure 3A**). In addition, this case had normal Rpt5-6, but very low or ND Rpt1-4.

Case 4 had aggregates of 70-kDa tau with full-length tau, Carboxyl-terminus truncated tau-aggregates, and 20-kDa mid-section tau-fragments aggregates of 0.45 AU. Case 4 had down regulated 20S α-subunits and β-subunits at 8% and 26%, respectively, of Case 1 (**Figure 2B**), and 11S α-subunits and 11S β-subunit monomers at 21% and 6%, respectively, of Case 1 (**Figure 3B**). Case 4 had over expression of Rpt1-2 and Rpt 6 at 2 to 3-fold higher levels than Case 1; however, Rpt4 was at 7% of Case 1, while Rpt3 and five were ND.

In summary, non-AD Cases 2-4 had undigested tau derived from incomplete degradation, but Case 1 contained ND tau and tau peptides. The 20S core, 11S proteasome and 19S base Rpt1-

6 were downregulated or occasionally over expressed in fewer irregular subunits than normal Case 1 (**Table 2**). The 11S monomer β-subunits are inhibitory on degrading tau peptides (**Table 3**).

Tau and proteasomal components in early AD and AD

Early AD (Cases 5-6) had undigested tau only, while Cases 7-16 contained both undigested tau and P-tau (**Table 2**). Among the undigested 70-kDa tau in 15 diseased cases, there were 13, 8 and 4, and 1 positive- blots of Amino-terminus, two mid-sections, and Carboxyl-terminus, while Case 1 lacked 70-kDa tau and 70-kDa P-tau (**Table 3**).

Early AD Cases 5-10 had downregulated 20S α-subunits and β-subunits (**Table 2**), and 11S α- and β-subunits as 30-kDa monomers (**Table 3**) and had impaired Rpt1-6 when compared to Case 1 (**Figure 4**). Case 8 had substantial levels of undigested tau and impaired 20S α-subunits

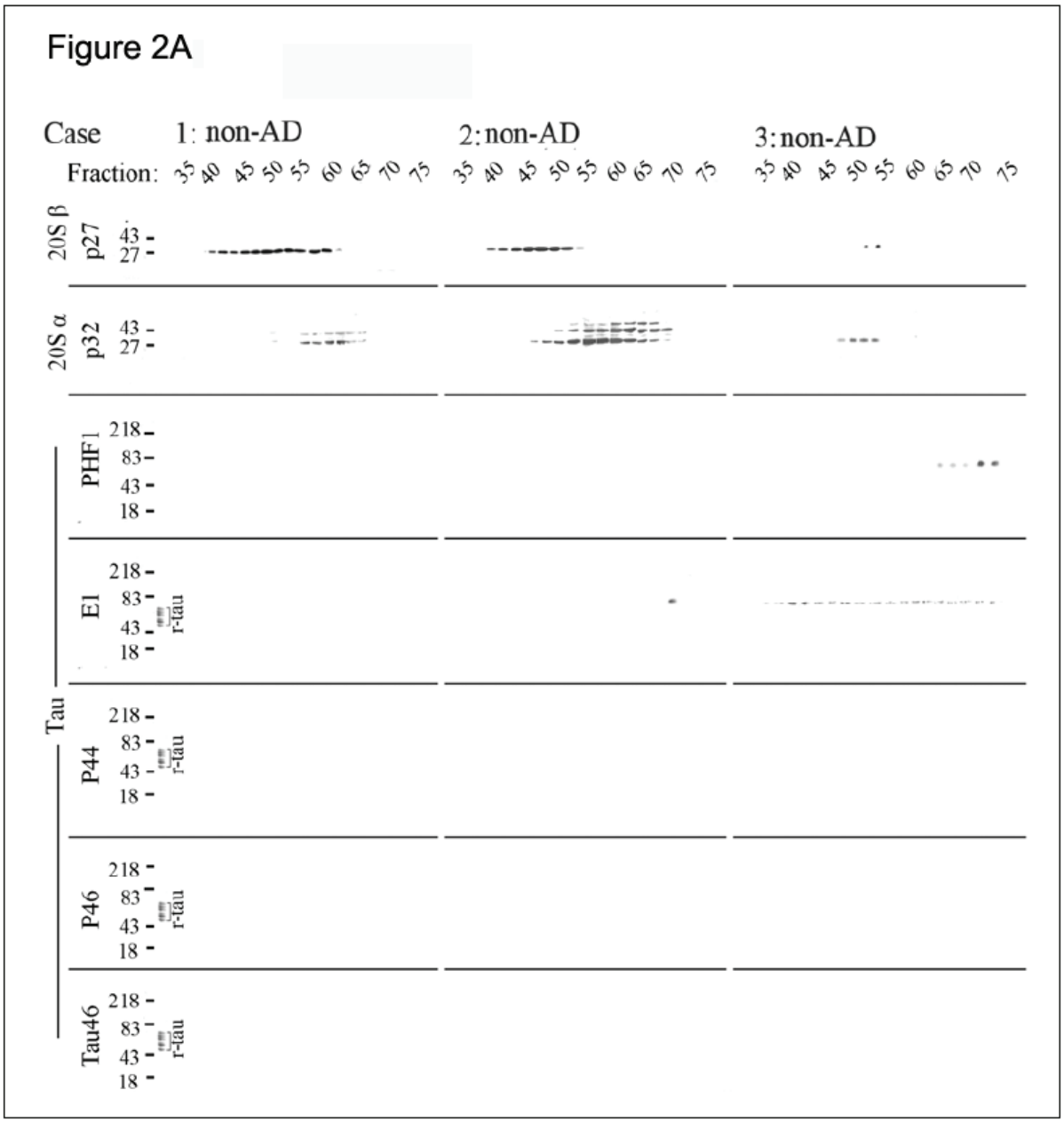

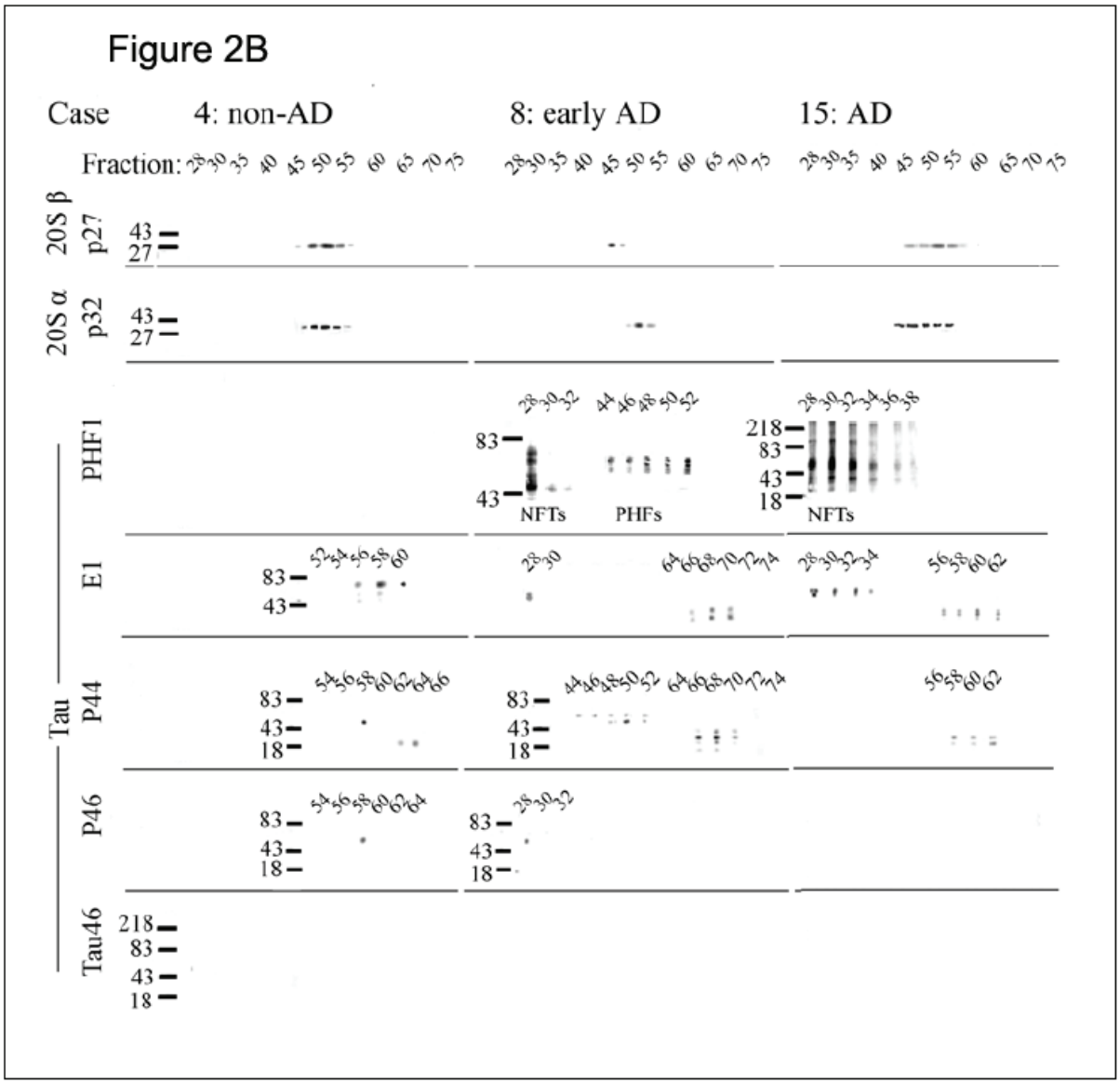

Figure 2A-2B. Six cases of tau and 20S proteasome core. Tau N-end, two mid-sections, and C-end epitopes were blotted with antibody E1, P44 and P46, and Tau46, and phosphorylated (P)-tau was probed by PHF1 antibody. The 20S α -subunits and β-subunits were detected using antibody p32 and p27, respectively. Levels of tau and 20S α-subunits and β-subunits on the blots were analyzed by densitometry. Case 1 has not detectable (ND) tau and ND P-tau that are valued at zero. γ-tau: recombinant-tau.

and β-subunits at 26% and 8%, respectively, (**Figure 2B**) of Case 1 as well as defective 11S monomer α-subunits and ND β-subunits (**Figure 3B**). The tauopathy was indicated by several lines of evidence. We detected the presence of developing PHF-tau within F28-32, where F30 and F32 contained P-tau aggregates in which F30 had 3.6-fold higher levels than F32. F28 had several advanced 78-48-kDa P-tau aggregates, with the top one containing full-length tau that blotted positive for the Amino-terminus and/or mid-section. PHF-tau of 70-kDa were also detected in F44-F52 between P-tau and full -length tau and positive in blots of tau mid-section. Small tau fragments at 42-28-kDa in F56-F62 contained the Amino-terminus and/or

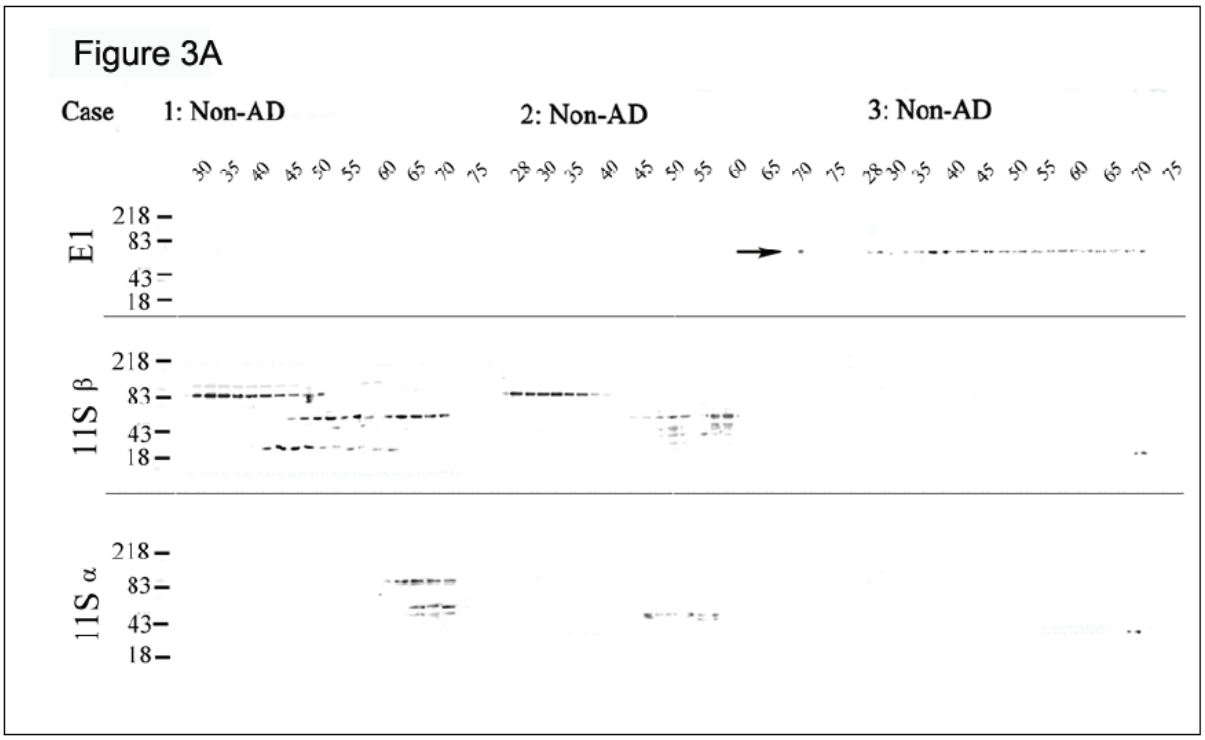

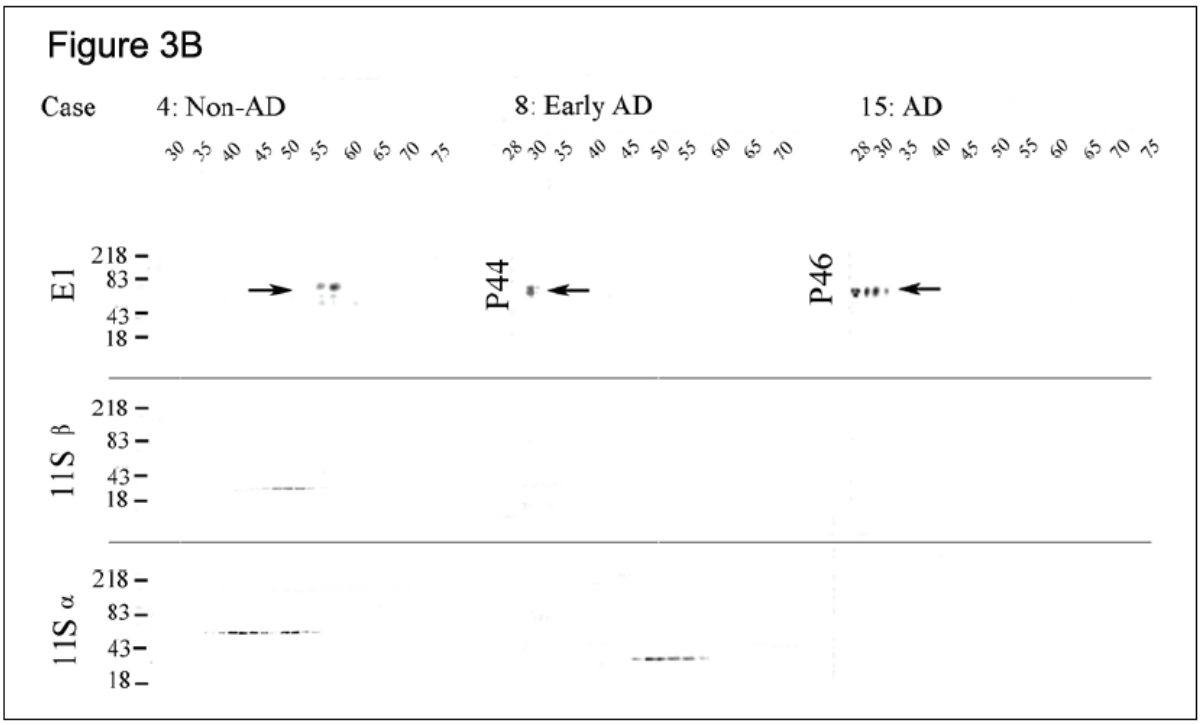

Figure 3A-3B. Six cases of 70kDa tau and 11S proteasome. 70kDa tau was dissected at a level above the 4R-2N isomer (68kDa) from the tau blots. 11S α-subunits and β-subunits were blotted by 11S α and β antibody. 11S subunits consist of 90kDa trimers and 60kDa dimers and 30kDa monomers: the two oligomers are stimulatory and the monomer is inhibitory in function. Case 1 had ND 70kDa tau that was valued at zero.

mid-section (**Figure 2B**). Case 6 had Rpt1-6 expression between 2% and 70% of Case 1, and Case 10 possessed Rpt1-6 between 0 to 83% of Case 1 (**Figure 4**).

AD (Cases 11-16) had marked undigested tau and P-tau, impaired proteasome profiles of 20S α-subunits and β-subunits (**Table 2**), 11S α-subunits and β-subunits represented as 30--kDa monomers (**Table 3**) and uncoordinated Rpt1-6 expression (**Figure 4**) as compared with Case 1. Case 15 had severe tauopathy, down-regulated 20S α-subunits and β-subunits (**Figure 2B**) as well as 11S α-subunits and β-subunits (**Figure 3B**) and defective Rpt1-6 as compared with Case 1. The case had very high NFT-tau in F28-F38 and tau-fragments in F56--F62 (**Figure 2B**). A full spectrum of NFT-tau included tau fragments, full-length tau with exposed amino-terminus and/or mid-sections and high MW tau aggregates that accounted for 16%, 57% and 27%, respectively, of the accumulating P-tau (**Figure 2B**). This case also had impaired Rpt1-6 at 0 to 71% of Case 1 (**Figure 4**).

Correlation studies

When the four non-AD cases were considered together, levels of tau and 20Sβ-subunits (**Table 2**) as well as 70-kDa tau and 11Sβ-subunits (**Table 3**) had significant inverse relationships of R= -0.95 (upper panel, **Figure 5A**) and R= -0.97 (upper panel, **Figure 5B**), respectively. The trends remain constant whether all four cases or only Cases 2 to 4 were included in the regression analysis. These trend lines show that as the levels of 20S β-subunits and 11S β-subunits increase, levels of tau and tau peptides decrease until they become ND.

When all 16 cases were considered together, levels of tau and 20S β-subunits (**Table 2**) as well as 70-kDa tau and 11S β-subunits (**Table 3**) had significant inverse relationships {P<0.005 and R= -0.49 (lower panel, **Figure 5A**); and P<0.05 and R= -0.44 (lower panel, **Figure 5B**)}, respectively. Both Figures show two phases: a steep decline of substrate tau and tau-peptides degraded by effective 20S β-subunits and 11S β-subunits; and a stable accumulation of tau and tau-peptide caused by impaired 20S β-subunits and 11S β-subunits. However, there was no significant inverse correlation between the levels of P-tau and 20S β-subunits or between 70-kDa P-tau and 11S β-subunits (data not shown).

Undigested tau accumulation

The undigested tau increased from ND in Case 1 to 0.040 ± 0.011 AU in non-AD disease controls Cases 2-4, 0.379 ± 0.144 AU in early-AD Cases 5-10, and 0.449 ± 0.097 AU in AD Cases 11-16 (**Table 2**). The levels of Carboxyl-terminus truncated tau between early AD and AD cases are significant {P<0.02 (#, **Figure 6**)}, and the levels of the carboxyl-terminus and mid-section of tau in 16 cases are significant {P<0.007 (*, **Figure 6**)}. However, levels of P-tau elevated from ND in Case 1, to 0.019 AU in non-AD Case 3, to 0.102 ± 0.046 AU in early AD, and to 1.660 ± 1.024 AU in AD (**Table 2**). Levels of P-tau between early AD and AD cases are significant {P<0.04 (++, **Figure 6**)}, and levels of tau and P-tau in 16 cases are significant {P<0.02 (**, **Figure 6**)}.

Proteasomal 20S β-protease activity level

Using fluorescence substrate assay we determined that 20S β-proteases in Case 1 had chymotrypsin (12,024FU), trypsin (75,897FU) and caspase activity (69,543FU) of moderate and coordinated expression and that the chymotrypsin activity had the lowest Km. The indices of the three β-proteases in Case 1 were all set to 1.00 for normalization. Consequently, the average index of chymotrypsin had increased from normal at 1.00 to 1.90 ± 0.94 (n=3) in diseased non-AD Cases, to 8.08 ± 4.28 (n=6) in early AD and to 14.8 ± 5.70 (n=6) in AD. The average index of trypsin was altered from normal at 1.00 to non-AD at 0.51 ± 0.33, to early-AD at 1.39 ± 0.43 and to AD at 1.75 ± 0.62. The average index of caspase changed from normal at 1.00 to non-AD at 0.87± 0.34, to Early-AD at 0.70 ± 0.33 and to AD at 0.67 ± 0.13, respectively (**Table 4**).

Correlations of tau and 20S β-proteases

In 16 cases, significant relationships exist between levels of tau and index of 20S-chymotrypsin, P<0.007; indexes of chymotrypsin + trypsin, P<0.005; chymotrypsin + caspase, P<0.009; and all β-protease, P <0.009. All of the correlations seemed to be driven by chymotrypsin activity (**Figure 7**). No correlation was found between levels of tau and trypsin or cas-

Figure 4

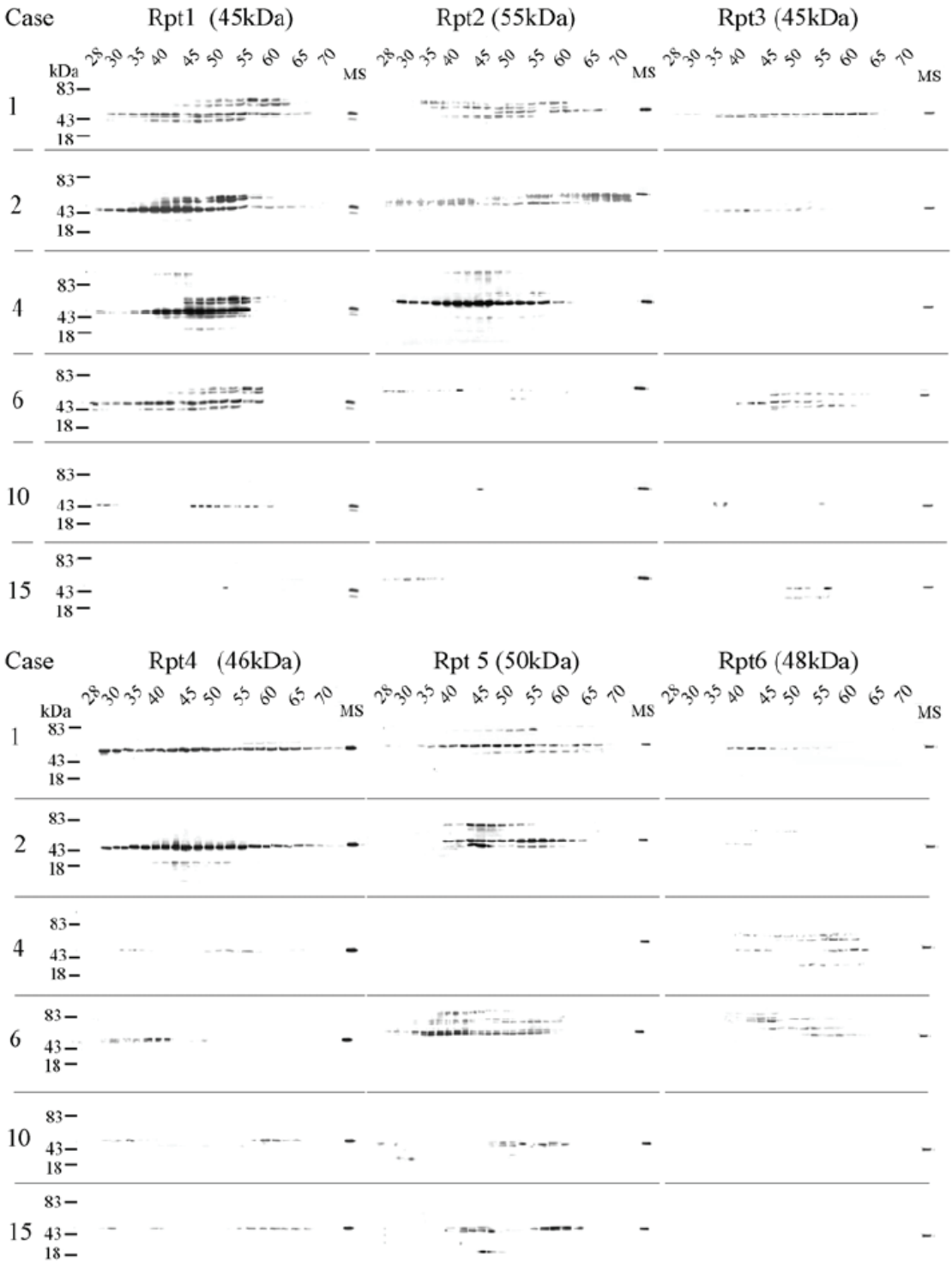
Case
Rpt1 (45kDa)
Rpt2 (55kDa)
Rpt3 (45kDa)
kDa
28 30 35 40 45 50 55 60 65 70 MS
1
2
4
6
10
15
83
43
18
Case
Rpt4 (46kDa)
Rpt 5 (50kDa)
Rpt6 (48kDa)

Figure 4. Six cases of 19S base Rpt1-6. Characteristics of Rpt1-6 are featured in six cases. Case 1 has a normal proteasome profile including well expressed Rpt1-6 demonstrated by ND tau for complete tau degradation and is regarded as a paradigm case. The remaining 15 cases contain abnormal proteasome profiles including impaired Rpt1-6 and are considered as diseased cases. MS: Subunit molecular standard.

pase. There were also no correlations between P-tau and any 20S β-protease.

Size-exclusion chromatography (SEC)

The resolution of cytosolic tau in SEC was shown (**Figure 8**). The resolution of SEC is accurate above 43 Å or 50-kDa. Highly purified PHF and the r-tau were resolved at F44 (71 Å, 959-kDa) and F59 (49 Å, 236-kDa), respectively. In addition, the earliest PHF1 positive P-tau in F28 -38 shown in tall smear columns was identified as NFTs. Each protein resolved in the SEC fraction had Rs and MW values that corresponded to their fraction. Furthermore, the resolved proteins were stable when stored at -20°C without any indication of aggregation or degradation.

Discussion

This study was designed to examine the role of the proteasome in the degradation of tau and in the pathogenesis of progressive tauopathy in AD by examining brains with a wide range of tau pathology while simultaneously assessing tau and proteasomal subunits in tissue fractions separated by molecular mass using SEC. A comprehensive study such as this has not been previously reported. The study began by examining blots of purified cytosolic tau from brain samples using four antibodies to detect the amino-terminus through the mid-sections to the car-

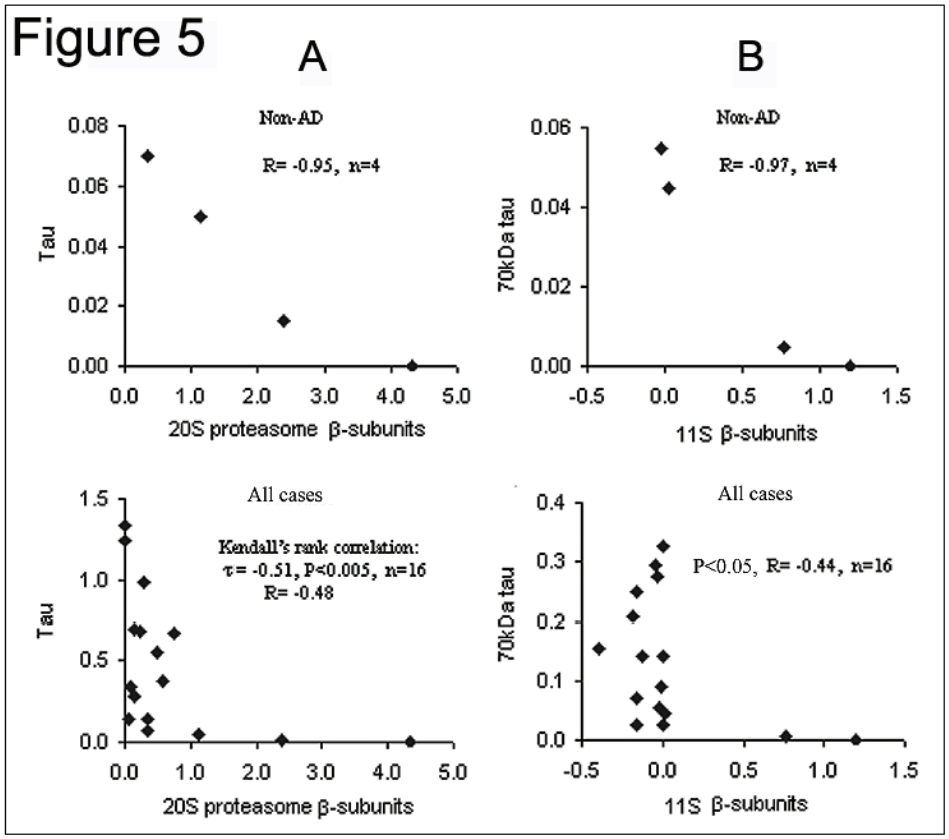

Figure 5. Correlations of tau and 20S β-subunits; and 70kda tau and 11S β-subunits. Levels of tau and 20S β-subunits (**A**) and 70kDa tau and 11S β-subunits (**B**) have significant inverse relationships: upper panels for four non-AD cases and lower panels for all 16 cases. Case 1 has ND tau and ND 70kDa tau that were valued at zero.

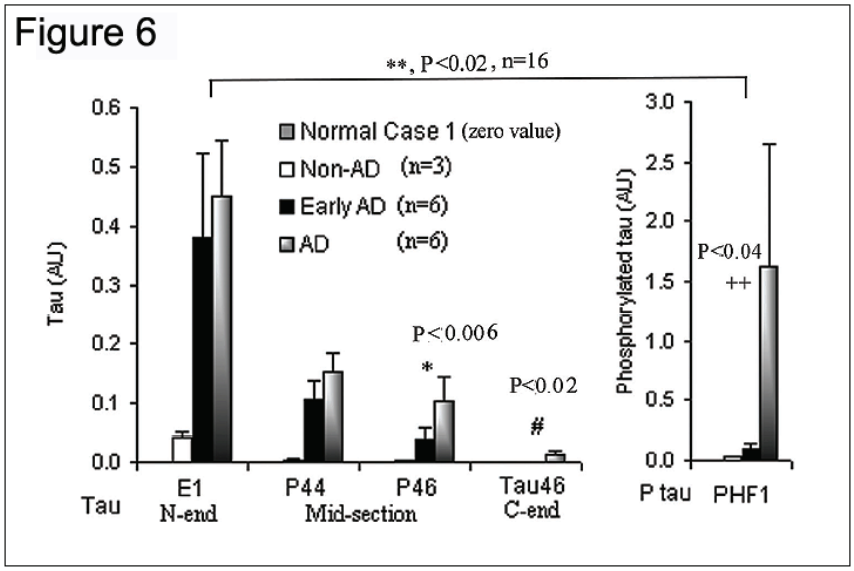

Figure 6. Characteristics of undigested tau in 16 cases. Levels of brain cytosolic tau N-end, two mid-sections, and C-end and P-tau were blotted and determined. Significant relationships are found: *, between the levels of C-end truncated tau between early AD and AD cases (n=6), P<0.02; ++, the levels between C-end and next mid-section of tau in 16 cases, P<0.006; #, the levels of P tau between early A D and AD cases (n=6), P<0.04; **, the levels between tau and P tau in 16 cases, P<0.02. Case 1 has ND tau that is valued at zero.

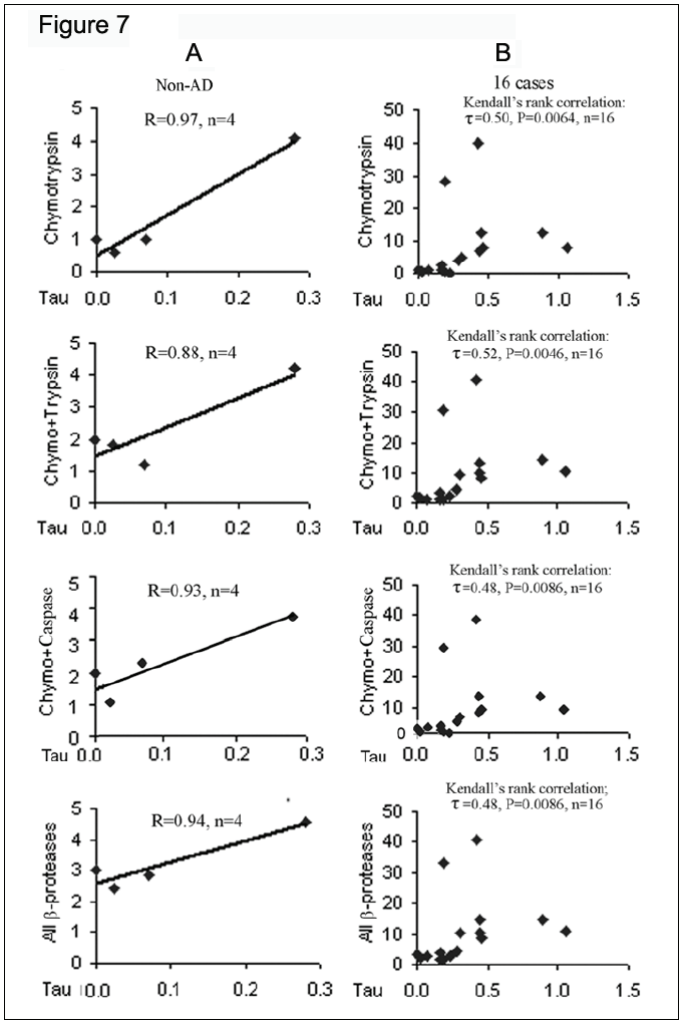

Figure 7. Correlations of tau and 20S proteasome β-proteases Levels of tau and 20S chymotrypsin, trypsin and caspase were analyzed by WB and FSA, respectively. Case 1 has all three indexes of β-proteases at 1.00 and Cases 2-16 have three indexes of β-proteases at various values. Significant relationships exist between the levels of tau and 20S chymotrypsin, P<0.007; chymotrypsin + trypsin, P<0.005; chymotrypsin + caspase, P<0.009; and all β-protease, P<0.009. Chymotrypsin: β_5 chymotrypsin-like; trypsin: β_2 trypsin-like; caspase: β_1 caspase-like. **A**: non-AD cases; **B**: 16 cases.

boxyl-terminus of tau. The blots were used to determine whether tau was completely degraded, as evidenced by inability to detect tau in normal brains, or incompletely degraded, as characterized by accumulation of undigested tau in aging and AD. Next, the levels of tau were correlated with levels of the 20S β-subunits and levels of 70-kDa tau were correlated with 11S β-subunits, which showed the efficacy of tau degradation by the proteasome. The results suggest that tau is degraded completely by the proteasome in controls and digested incompletely by the proteases in AD. This investigation, using autopsied human brains, may provide significant insight into tau metabolism in AD patho-

Figure 8

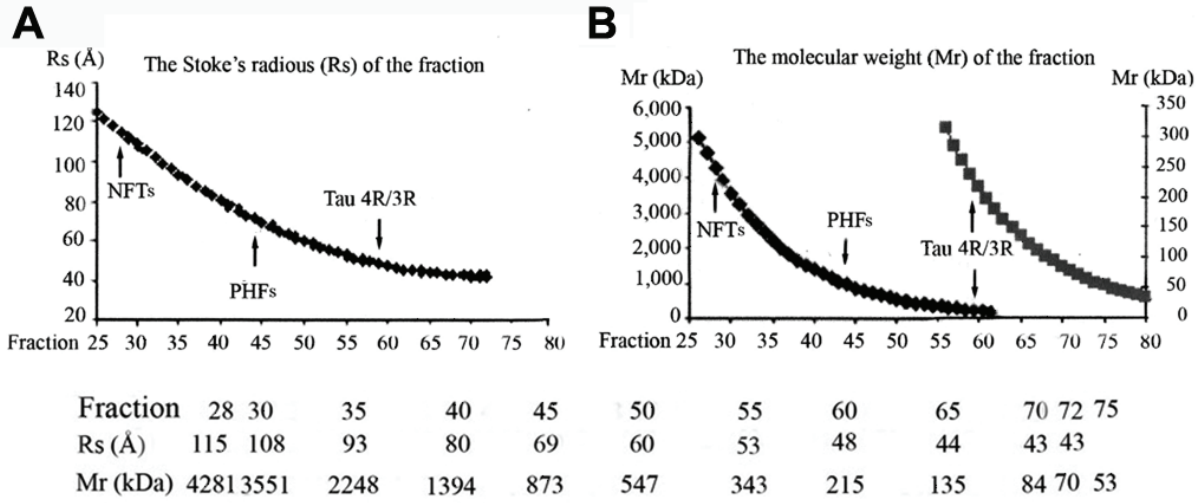

Fraction	28	30	35	40	45	50	55	60	65	70	72	75
Rs (Å)	115	108	93	80	69	60	53	48	44	43	43	
Mr (kDa)	4281	3551	2248	1394	873	547	343	215	135	84	70	53

Figure 8. Superose 6 size-exclusion chromatography (SEC). SEC was packed and calibrated using a high molecular weight kit and purified PHF preparation and stock recombinant (r)-tau. The NFTs were resolved at fraction (F) 28 (115 Å, 4,300 kDa). Both PHFs and full-length 3R/4R r-tau peaked at F44 (83 Å, 1,531 kDa) and F59 (49 Å, 236 kDa), respectively. A: the Stoke's radius of the protein (Rs, Å) and B: the MW (kDa).

genesis.

In a parallel study we previously studied tau pathology in 30 prospectively followed patients from the Mayo Clinic Alzheimer Disease Research Center grouped by cognitive impairment. Six cases in each of five Clinical Dementia Ratings scores - normal CDR (0), very mild (0.5), mild (1), moderate (2) and severe (3) were grouped firstly introduced by Morris [37] to differentiate the relative severity of dementia. The distribution of undigested tau was studied in temporal and frontal cortical tissue samples. One case with low CDR had ND tau and P-tau in both temporal and frontal cortices and four cases with low CDR had ND tau or P-tau in frontal cortices alone, which suggests that in cognitively normal elderly tau can be completely degraded. The data reiterate the view that the complete degradation of tau occurs normally and is not an isolated event. It probably occurs in most young brains and in cognitively intact elderly, while most elderly people with varying degrees of Alzheimer-related cognitive impairment have varying degrees of accumulation of undigested tau.

The hypothesis that levels of tau in the cytosol are normally tightly controlled and completely degraded if not associated with MT is new, but supported by the present results. This concept argues against the existing view of a tau pool present in the cytosol from which it is dispatched to stimulate assembly and stabilize MT. No mechanisms for tau storage and relocation have been demonstrated to support the presence of a stable pool of cytosolic tau. The evidence reported here suggests that tau is degraded completely in tissue that has a full complement of proteasomal components and normal enzymatic activity and that it accumulates progressively in association with aberration in this degradation process as incompletely digested or undigested tau that culminated in very large tau aggregates in full-blown AD. Thus, maintenance of a functional proteasome system to degrade cytosolic tau that is not bound to MT is important for optimal longevity in humans.

Tau that is not digested by proteases contains an intact amino-terminus, an irregular configured projection domain beyond the reach of proteases. Tau that accumulates during the progression of AD may be related to failure of the proteasome to completely degrade tau. It seems likely that there are factors, such as transcription factors, that induce enzymes (e.g., 20S

β-proteases) to clear tau and maintain homeostasis. In this study, levels of tau and 20S β-proteases were significantly correlated, perhaps indicative of an end-product induction mechanism. In order to be functional, the induced 20S β-proteases must integrate a complete core 20S α-ring template [20]. Both the 20S β-subunits and 20S β-proteases were closely distributed in SEC fractions in our reference case (Case 1), but not in SEC fractions from cases with progressive tauopathy (Cases 2-16). In these cases, the blots of 20S α-subunits were also abnormal. It is tempting to speculate that this pattern on SEC suggests that in the reference case 20S β-proteases successfully integrates into the core α-ring, but that the dispersion seen in SEC of the remaining cases indicates that integration is less successful, leaving ring elements within soluble cytosolic fractions.

The most significant finding in this study is the progressive failure of intrinsic mechanisms to degrade tau in AD. Undigested tau accumulates at first as soluble protein in the cytosol, with subsequent conversion without hyperphosphorylation to a form that is sarkosyl-soluble and then into a form that is sarkosyl-insoluble. This was noted in non-AD disease controls (Cases 2-4) and early AD (Cases 5-6), which all had undigested tau without significant P-tau. Truncated tau may compete with normal full-length tau for binding sites on MT that might cause destabilization of MT and subsequent deleterious effects on neurons. The intrinsic electrostatic forces in undigested tau and the enriched hydrophobicity in the MT-binding domains may create non-phosphorylated spatial epitopes that favor aggregation [8, 38, 39].

The proteasome is distributed mostly on the cytosolic surface of the ER and to a small extent within the nuclei [34]. The system consists mainly of 20S core, 11S and 19S proteasome activators (**Figure 1**). The firmly bound 20S core β-proteases interact by overlapping with opposite counterparts to cleave allosterically the peptide bonds for precise proteolysis. Levels 20S β-subunits were inversely related to tau in human brain tissue, suggesting that tau is a substrate of the proteasome. In addition, levels of 11S β-subunits were inversely correlated to the levels of 70-kDa tau in brain. The case with the most significant amounts of undigested tau (case 16) had the most abnormal proteasome profile. Among controls, Case 1, which was the reference case with the most complete proteasome profile, had no detectable tau, while a non-AD control with accumulation of 70-kDa tau (Case 2), had an abnormal proteasome profile. The results suggest that critical impairment of brain 20S β-subunits and 11S β-subunits during the aging process may contribute to accumulation of undigested tau and eventual neurofibrillary degeneration.

The 19S base Rpt1-6 that possesses chaperone-like activity helps to unfold proteins [27]. Rpn10 binds specifically to polyubiquitin chains attached to the substrate protein and assists in its unfolding to a susceptible form for degradation. Collectively, Rpt1-6, Rpn10 and Rpn2 in the 19S proteasome base recognize the substrate, unfold and facilitate the process of degradation [17]. The step of unfolded protein entry via an orifice of 20S α-ring to the antechamber and the central enzyme cavity for degradation is rate limiting [21, 23]. Degradation of proteins in the enzyme cavity is processive [40], whereby the substrate is held until completion and end products are released before accepting the next substrate. Overall, the proteasome degrades cytosolic proteins completely [26].

Previous studies by David et al. demonstrated that purified 20S proteasome core could degrade recombinant-tau to the intermediates of 17-26-kDa and 10-15-kDa or smaller peptides with extended incubation [12]. The 20S core degrades tau to peptides in an ubiquitin-independent manner. Evaluation of ubiquitination of tau in these cases would provide additional information about whether observed correlates between levels of tau and proteasomal subunits is ubiquitin-independent or rather dependent upon ubiquitination and consequently requiring energy (i.e. ATP-dependent).

Kisselev et al. proposed a bite-chew mechanism of 20Score degradation on short-lived proteins [24]. Chymotrypsin active sites “bite” and cleave various substrates to intermediates, and three active sites “chew” or cleave the intermediates to peptides; the 20S proteasome or peptidases rapidly reduce the peptides to amino acids. The two chymotrypsin sites may cleave a tau molecule to three tau intermediates, leaving the three β-protease sites to digest the intermediates to tau-peptides, followed quickly by reduction to amino acids or short antigen peptides by the 20S proteasome. A hybrid 26S pro-

teasome (19S-20S core-11S) degrades proteins, such as tau, to amino acids directly and/or antigen peptides [41]. Thus, the complete proteasomal degradation of tau is likely achieved by the combined effort of non-redundant subunits.

This study included advanced AD cases that had high density of neurofibrillary degeneration and massive accumulation of NFT tau. It is tempting to speculate, given the considerable aberration of proteasomal profiles in these cases, that NFT-tau is related to impaired 30S proteasome and 26 hybrid proteasome activity on degradation of tau. One case in particular (Case 15) had the massive NFT-tau as indicated by distribution in SEC to F28-F38 (**Figure 2B**). Such tau aggregates could easily exceed 115 Å and have molecular mass of 4,280-kDa or more (**Figure 2B**). The 20S core has a size of 12 nm in diameter and 17 nm in height [16, 18]; the proteasome has an estimated Rs of 102 Å, while full-length tau in F59 has an Rs of 49Å. The exact mechanism of NFT formation has not been elucidated; however, it is reasonable to suggest that large pathologic tau assemblies could block the enzyme cavity of 20S core and lead to a standstill of proteasomal degradation. Failure of 20S proteasome degradation of tau {see Case 8 with PHF-tau in F44-F52 (**Figure 2B**)} would lead to accumulation of abnormal P-tau of estimated molecular weight of 72-56kDa, far smaller than the massive P tau-aggregates (over 240-kDA) that probably correlated with NFT. Whether these smaller P-tau species have inherent toxicity remains to be determined, but might fit with the increasingly popular notion that toxic species in Alzheimer's disease are soluble oligomers, some derived from aberrant proteolytic processes [42, 43].

Acknowledgments

I am deeply indebted to Drs. Dennis W. Dickson and Shu-Hui Yen for their guidance and unwavering support during this project. Highly purified human PHF preparation and PHF1 antibody were provided by Dr. Peter Davies (Albert Einstein College of Medicine, Bronx, NY) and Tau46 antibody by Dr. V. M-Y. Lee (University of Pennsylvania, Philadelphia, PA). Autopsied human materials were obtained from Dr. Dickson and cases were obtained from ethically approved procedures by the Mayo IRB. The author has completed the education and examination required by Mayo IRB for handling of human specimens. The funding was provided by the Mayo Foundation for Medical Education and Research. Figures of the proteasome in **Figure 1** are from Tanahashi N, Murakami Y, Minami Y, Shimbara N, Hendil KB and Tanaka K. [44], reproduced with permission from the *Journal of Biological Chemistry*.

Address correspondence to: Samuel S. Yen, PhD, Department of Neuroscience, Mayo Clinic College of Medicine, 4500 San Pablo Road, Jacksonville, FL 32224, Tel: 904-953-2585 or 1066 Fax: 904-953-7117 E-Mail: yen.samuel@mayo.edu

References

[1] Minati L, Edginton T, Bruzzone MG and Giaccone G. Current concepts in Alzheimer's disease: a multidisciplinary review. Am J Alzheimers Dis Other Demen 2009; 24: 95-121.

[2] Lee VM, Balin BJ, Otvos L, Jr and Trojanowski JQ. A68: a major subunit of paired helical filaments and derivatized forms of normal Tau. Science 1991; 251:675-678.

[3] Grundke-Iqbal I, Iqbal K, Quinlan M, Wisniewski H and Binder L. Microtubule-associated protein tau. A component of Alzheimer paired helical filaments. J Biol Chem 1986; 261: 6084-6089.

[4] Wischik CM, Novak M, Edwards PC, Klug A, Tichelaar W and Crowther RA. Structural characterization of the core of the paired helical filament of Alzheimer disease. Proc Natl Acad Sci U S A 1988; 85: 4884-4888.

[5] Selkoe DJ, Ihara Y and Salazar FJ. Alzheimer's disease: insolubility of partially purified paired helical filaments in sodium dodecyl sulfate and urea. Science 1982; 215:1243-1245.

[6] Yen S S, Ishizawa T, Dickson D W, Boeve B, Knopman D, Smith G, Ivnik R, Peterson R, Lee G and Yen S-H. Correlation of tau and cognition in prospectively studied elderly humans. Neurobiol Aging 2002; 23: S490-491.

[7] Goedert M, Wischik CM, Crowther RA, Walker JE and Klug A. Cloning and sequencing of the cDNA encoding a core protein of the paired helical filament of Alzheimer disease: identification as the microtubule-associated protein tau. Proc Natl Acad Sci U S A 1988; 85: 4051-4055.

[8] Jeganathan S, von Bergen M, Brutlach H, Steinhoff HJ and Mandelkow E. Global hairpin folding of tau in solution. Biochemistry 2006; 45: 2283-2293.

[9] Brandt R, Leger J and Lee G. Interaction of tau with the neural plasma membrane mediated by tau's amino-terminal projection domain. J Cell Biol 1995; 131:1327-1340.

[10] Rendon A, Jung D and Jancsik V. Interaction of microtubules and microtubule-associated proteins (MAPs) with rat brain mitochondria. Biochem J 1990; 269: 555-556.

[11] Loomis PA, Howard TH, Castleberry RP and Binder LI. Identification of nuclear tau isoforms in human neuroblastoma cells. Proc Natl Acad Sci U S A 1990; 87: 8422-8426.
[12] David DC, Layfield R, Serpell L, Narain Y, Goedert M and Spillantini MG. Proteasomal degradation of tau protein. J Neurochem 2002; 83:176-185.
[13] Kenessey A, Nacharaju P, Ko LW and Yen SH. Degradation of tau by lysosomal enzyme cathepsin D: implication for Alzheimer neurofibrillary degeneration. J Neurochem 1997; 69: 2026-2038.
[14] Canu N, Dus L, Barbato C, Ciotto MT, Brancolini C, Rinaldi AM, Novak M, Cattaneo A, Bradbury A and Calissano P. Tau cleavage and dephosphorylation in cerebellar granule neurons undergoing apoptosis. J Neurosci 1998; 18: 7061 -7074.
[15] Yen SS, Easson C, Nacharaju P, Hutton M and Yen SH. FTDP-17 tau mutations decrease the susceptibility of tau to calpain I digestion. FEBS Lett 1999; 461: 91-95.
[16] Carrard G, Bulteau AL, Petropoulos I and Friguet B. Impairment of proteasome structure and function in aging. Int J Biochem Cell Biol 2002; 34:1461-1474.
[17] Baumeister W, Walz J, Zuhl F and Seemuller E. The proteasome: paradigm of a self-compartmentalizing protease. Cell 1998; 92: 367-380.
[18] Bochtler M, Ditzel L, Groll M, Hartmann C and Huber R. The proteasome. Annu Rev Biophys Biomol Struct 1999; 28: 295-317.
[19] Coux O, Tanaka K and Goldberg AL. Structure and functions of the 20S and 26S proteasomes. Annu Rev Biochem 1996; 65: 801-847.
[20] Groll M, Heinemeyer W, Jager S, Ullrich T, Bochtler M, Wolf DH and Huber R. The catalytic sites of 20S proteasomes and their role in subunit maturation: a mutational and crystallographic study. Proc Natl Acad Sci U S A 1999; 96:10976-10983.
[21] Heinemeyer W, Fischer M, Krimmer T, Stachon U and Wolf DH. The active sites of the eukaryotic 20 S proteasome and their involvement in subunit precursor processing. J Biol Chem 1997; 272: 25200-25209.
[22] Heinemeyer W, Trondle N, Albrecht G and Wolf DH. PRE5 and PRE6, the last missing genes encoding 20S proteasome subunits from yeast? Indication for a set of 14 different subunits in the eukaryotic proteasome core. Biochemistry 1994; 33:12229-12237.
[23] Jager S, Groll M, Huber R, Wolf DH and Heinemeyer W. Proteasome beta-type subunits: unequal roles of propeptides in core particle maturation and a hierarchy of active site function. J Mol Biol 1999; 291: 997-1013.
[24] Kisselev AF, Akopian TN, Castillo V and Goldberg AL. Proteasome active sites allosterically regulate each other, suggesting a cyclical bite-chew mechanism for protein breakdown. Mol Cell 1999; 4: 395-402.
[25] Kisselev AF, Akopian TN, Woo KM and Goldberg AL The sizes of peptides generated from protein by mammalian 26 and 20 S proteasomes. Implications for understanding the degradative mechanism and antigen presentation. J Biol Chem 1999; 274: 3363-3371.
[26] Yewdell JW. Not such a dismal science: the economics of protein synthesis, folding, degradation and antigen processing. Trends Cell Biol 2001; 11: 294-297.
[27] Wolf S, Nagy I, Lupas A, Pfeifer G, Cejka Z, Muller SA, Engel A, DeMot R and Baumeister W. Characterization of ARC, a divergent member of the AAA ATPase family from Rhodococcus erythropolis. J Mol Biol 1998; 277:13-25.
[28] Bandyopadhyay B, Li G, Yin H and Kuret J. Tau aggregation and toxicity in a cell culture model of tauopathy. J Biol Chem 2007; 282: 16454-16464.
[29] Crowe A, Ksiezak-Reding H, Liu WK, Dickson DW and Yen SH. The N terminal region of human tau is present in Alzheimer's disease protein A68 and is incorporated into paired helical filaments. Am J Pathol 1991; 139: 1463-1470.
[30] Liu WK, Dickson DW and Yen SH. Heterogeneity of tau proteins in Alzheimer's disease. Evidence for increased expression of an isoform and preferential distribution of a phosphorylated isoform in neurites. Am J Pathol 1993; 142: 387-394.
[31] Liu WK, Dickson DW and Yen SH. Amino acid residues 226-240 of tau, which encompass the first Lys-Ser-Pro site of tau, are partially phosphorylated in Alzheimer paired helical filament-tau. J Neurochem 1994; 62:1055-1061.
[32] Liu WK, Moore WT, Williams RT, Hall FL and Yen SH. Application of synthetic phospho- and unphospho- peptides to identify phosphorylation sites in a subregion of the tau molecule, which is modified in Alzheimer's disease. J Neurosci Res 1993; 34: 371-376.
[33] Ksiezak-Reding H, Chien CH, Lee VM and Yen SH. Mapping of the Alz 50 epitope in microtubule-associated proteins tau. J Neurosci Res 1990; 25: 412-419.
[34] Peters JM, Franke WW and Kleinschmidt JA. Distinct 19 S and 20 S subcomplexes of the 26 S proteasome and their distribution in the nucleus and the cytoplasm. J Biol Chem 1994; 269: 7709-7718.
[35] Dubiel W, Pratt G, Ferrell K and Rechsteiner M. Purification of an 11 S regulator of the multicatalytic protease. J Biol Chem 1992; 267: 22369-22377.
[36] O'Brien MA, Moravec RA, Riss TL and Bulleit RF. Homogeneous, bioluminescent proteasome assays. Methods Mol Biol 2008; 414:163-181.
[37] Morris JC. The Clinical Dementia Rating (CDR): current version and scoring rules. Neurology 1993; 43: 2412-2414.

[38] Kampers T, Friedhoff P, Biernat J, Mandelkow EM and Mandelkow E. RNA stimulates aggregation of microtubule-associated protein tau into Alzheimer-like paired helical filaments. FEBS Lett 1996; 399: 344-349.
[39] Ksiezak-Reding H and Yen SH. Structural stability of paired helical filaments requires microtubule-binding domains of tau: a model for self-association. Neuron 1991; 6: 717-728.
[40] Akopian TN, Kisselev AF and Goldberg AL. Processive degradation of proteins and other catalytic properties of the proteasome from Thermoplasma acidophilum. J Biol Chem 1997; 272:1791-1798.
[41] Wenzel T and Baumeister W. Conformational constraints in protein degradation by the 20S proteasome. Nat Struct Biol 1995; 2: 199-204.
[42] De Strooper B Proteases and proteolysis in Alzheimer disease: a multifactorial view on the disease process. Physiol Rev 2010; 90: 465-494.
[43] Ferreira ST, Vieira MN and De Felice FG. Soluble protein oligomers as emerging toxins in Alzheimer's and other amyloid diseases. IUBMB Life 2007; 59: 332-345.
[44] Tanahashi N, Murakami Y, Minami Y, Shimbara N, Hendil KB and Tanaka K. Hybrid proteasomes. Induction by interferon-gamma and contribution to ATP-dependent proteolysis. J Biol Chem 2000; 275: 14336-14345.